

Regular Patterns of Cracks Formed by Directional Drying of a Colloidal Suspension

C. Allain

Laboratoire Fluides, Automatique et Systèmes Thermiques (URA CNRS 871), Bâtiment 502, Campus Universitaire, 91405 Orsay Cedex, France

L. Limat

Laboratoire de Physique et de Mécanique des Milieux Hétérogènes (URA CNRS 851), ESPCI, 75231 Paris Cedex 05, France
(Received 29 June 1994)

We studied the pattern of cracks formed during the drying of a colloidal suspension. Because of water evaporation, particles and ionic species accumulate near the surface and a gel forms and shrinks. In a confined geometry, the gel shrinkage leads to large stresses which are the cause of crack formation. For the 1D geometry used, we observe that the cracks are regularly spaced. Taking into account the competition between stress relaxation due to crack opening and stress increase due to water loss through the crack, we develop a simplified model which allows understanding of the observed pattern.

PACS numbers: 62.60.Mk, 47.20.Hw, 47.20.Ky, 82.70.Gg

In recent years, there has been much interest in crack formation and breaking phenomena. Several statistical models have been introduced to describe the failure of disordered solids [1,2]. A special case of great interest for practical applications is the rupture of surface layers which often occurs due to the mismatch between the elastic properties of the bulk matter and those of the film [3,4]. On the other hand, multiple crack growth caused by thermal shock has been investigated; in particular, the stability of the propagation of parallel crack penetrating a sample after quenching was analyzed [5–10]. These situations would constitute a model in fracture mechanics of the problem of the nonlinear dynamics of cellular structure which has been mainly investigated in hydrodynamics and in directional solidification [11].

In this Letter, we report the crack pattern formed by directional drying of thin colloidal suspension slabs. The cracks are all parallel to the drying direction and to the smallest dimension of the sample. We show that they form a periodic pattern with a wavelength increasing with the sample thickness. These observations are related to the fact that a crack constitutes a preferential path of evaporation. Using a scalar description of the mechanical properties and an analogy with a thermal problem, we calculate the stress field in a simplified 2D geometry. We show that the coupling between elasticity and diffusion leads to a well defined spacing between the cracks. Its variation as a function of the sample thickness is in qualitative agreement with the wavelength variation observed experimentally.

The experiments were carried out on thin parallelepiped cells made from two transparent glass slides of dimensions $26 \times 75 \text{ mm}^2$ (see Fig. 1). The two slides were first separated by Mylar spacers placed along the longest slide sides and then the two sides were sealed with epoxy. The other two sides were left open in order to fill the cell and allow evaporation to take place. Spacers of thick-

nesses varying from 15 to 100 μm were used. The final thickness of the cell e was controlled using a high-precision micrometer and the parallelism of the slides was determined by interferometric observations. The sample used was an aqueous colloidal silica suspension having a high particle volume fraction ($\Phi = 0.33$). The radius of the particles a , determined by electron microscopy, is $9 \pm 2 \text{ nm}$. The particle surface bears a high negative charge density (the pH is about 9.0); then, in the absence of evaporation the suspension is stable [12]. The cell was partially filled by capillary rise at about a 2 cm height and placed horizontally. Drying phenomena then begin. Near the inner meniscus, the air is rapidly saturated by water and evaporation stops. In contrast, near the outer meniscus, the water vapor is evacuated and the sample regularly loses water. So the particles accumulate near the open surface and since, at the same time, the ionic strength increases under our physiochemical conditions, a colloidal gel forms. Capillary tension induces water drainage to prevent exposure to air of the silica particle near the outer meniscus leading to the shrinkage of the gel [13]. Since the gel sticks on the cell glass plates, it results in large stresses which are at the

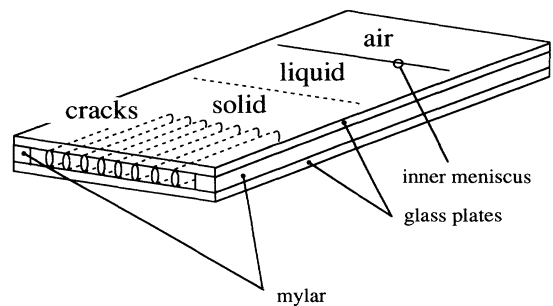


FIG. 1. Schematic of the cell used to observe directional drying.

origin of the crack formation. It is noteworthy that the temperature variation due to cooling by evaporation is very small (we can estimate it to 10^{-1} °C) and does not contribute significantly to the stresses. Finally, we observe that cracks nucleate very easily in this system. From the order of magnitude of the critical stress intensity factor $K_{IC} \cong 10^2 \text{ N m}^{-3/2}$ [14], we can estimate the stress required to develop a fracture from a flaw of typical size close to the size of the material inhomogeneities (of the order of the particle radius): $K_{IC}/\sqrt{\pi a} \cong 10^6 \text{ N m}^{-2}$. This value is smaller than the typical maximum stress induced by the embedded gel contraction $B\Delta\varphi_w \cong 6 \times 10^8 \text{ N m}^{-2}$, where $B \cong 2 \times 10^9 \text{ N m}^{-2}$ is the bulk modulus of the medium and $\Delta\varphi_w \cong 3 \times 10^{-1}$ the available volume fraction of water. In addition, $K_{IC}/\sqrt{\pi a}$ is also smaller than the capillary pressure drop, which is of the order of $2\gamma/a \cong 2 \times 10^7 \text{ N m}^{-2}$, where γ is the air-water interfacial tension.

Experimentally, we observe the formation of the first cracks about 10 min after the beginning of drying. Starting from the evaporation exposed surface, they penetrate the sample for about 1 mm. About 1 min later, a pattern of

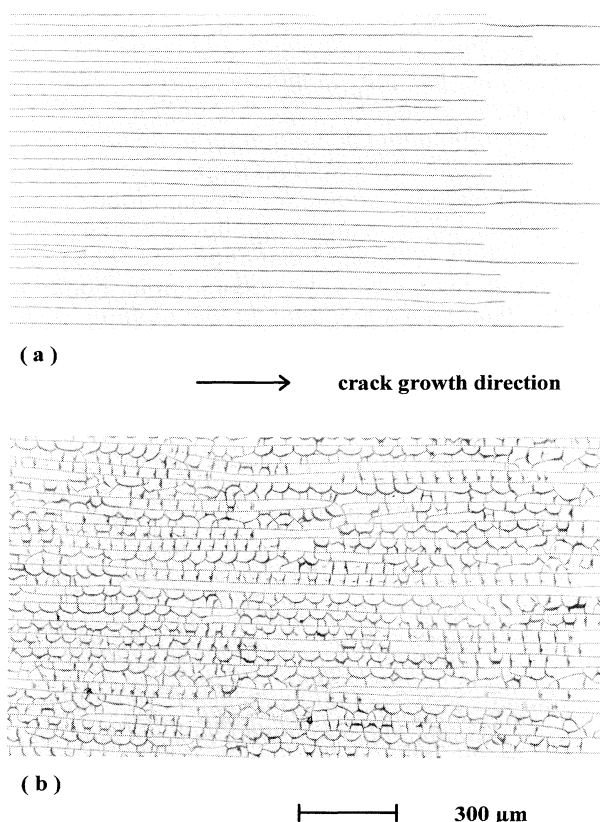


FIG. 2. Top views of the crack pattern: (a) crack front invading the cell, (b) secondary branching, taken about 10 min later. The evaporation side is on the left. The cell thickness is $15 \mu\text{m}$.

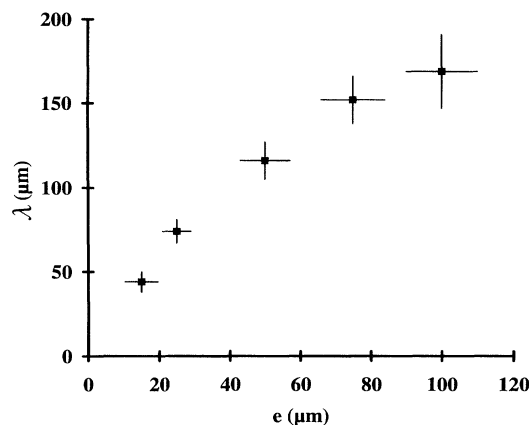


FIG. 3. Variation of the measured wavelength as a function of the cell thickness. The bars are the errors in the measurements.

cracks covers the whole width of the cell. Progressively, the cracks grow and invade all the sample as evaporation continues. Finally, multiple branching and fracture occur when the lost water volume becomes large. Figure 2 presents typical photographs of the observed crack pattern. When the sample thickness is increased above $\cong 150 \mu\text{m}$, the spatial repartition of the cracks is no longer unidimensional as fractures parallel to the open side form as the front moves. We measured the variation of the wavelength λ as a function of the sample thickness for $e \leq 100 \mu\text{m}$. As shown in Fig. 3, λ increases continuously with e ; its variation deviates only slightly from a simple linear increase.

To explain the periodicity of the patterns observed, we remark that the crack constitutes a preferential path of evaporation. So, although the stress is relaxed in the vicinity of a crack just after it opens, the stress reincreases with time due to water loss by the aperture. The superposition of the internal stress induced by water drainage on the crack-relaxed stress yields a maximum in the variation of the stress with the distance from the crack. It results that the next crack will form or grow at a well defined spacing from the initial crack. An exact determination of the stress field in the slab is difficult and would require numerical computations. To find the relevant parameters, we set up here a simplified model allowing a physical discussion. Considering only what occurs in a plane perpendicular to the direction of drying, we develop a 2D model. The x axis is chosen parallel to the glass-plates direction and the y axis perpendicular to it (see inset in Fig. 4). To calculate the stress field, we use a scalar model with a 1D displacement $u(x, y, t)$ parallel to the x axis [15], and the evolution of the water content is treated by analogy with the temperature variations in a nonisothermal problem [16]. Then the xx and xy stress component are given by $\sigma_{xx} = \tilde{E}[(\partial u/\partial x) + C]$ and $\sigma_{xy} = \tilde{E}(\partial u/\partial y)$ where \tilde{E} is the effective gel elastic modulus, and $\tilde{E}C$ is the internal stress created by the

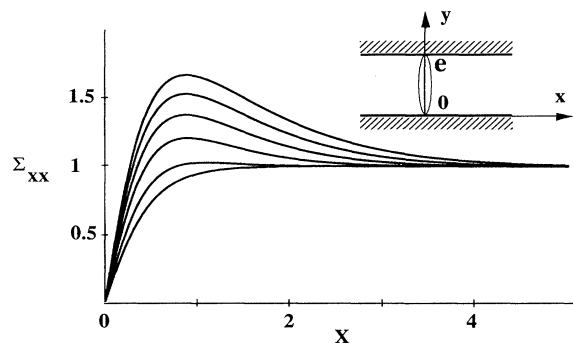


FIG. 4. Variation of the dimensionless stress $\Sigma_{xx} = \sigma_{xx}/\bar{E}C_\infty$ as a function of the dimensionless distance $X = x/e$ calculated for $Y = y/e = \frac{1}{2}$ and $K = 1$ and for different values of $T = Dt/e^2$. From down to up, $T = 0, 0.4, 0.8, 1.2, 1.6$, and 2 . Inset: coordinate system.

variations of the water volume: $C = (\varphi_w - \varphi_{w0})/\varphi_{w0}$, where φ_w is the water volume fraction, and φ_{w0} is the value of φ_w in the absence of gel shrinkage. The equilibrium relation can be expressed as $\partial\sigma_{xx}/\partial x + \partial\sigma_{xy}/\partial y = 0$, which leads to

$$\frac{\partial^2 u}{\partial x^2} + \frac{\partial^2 u}{\partial y^2} = -\frac{\partial C}{\partial x}. \quad (1)$$

It is noteworthy that this scalar description corresponds to an electric analogy of the elastic problem, u being the equivalent of the electrostatic potential, σ_{xx} and σ_{xy} of the currents on x and y , and $-\partial C/\partial x$ of a charge density.

Now let us assume that a crack perpendicular to the evaporation surface, i.e., to the plane x, y , forms at $t = 0$ in $x = 0$. As water is evacuated by the crack, C varies along x and, in the framework of the analogy with a thermal problem, the evolution of $C(x, t)$ is given by

$$\frac{\partial C}{\partial t} = D \frac{\partial^2 C}{\partial x^2}, \quad (2)$$

where the diffusion coefficient D is related to the transport of water through the porous medium that constitutes the silica gel [16]. The boundary conditions are no slip on the glass plates, $u = 0$ in $y = 0$ and no stress on the surface of the crack, $\sigma_{xx} = 0$, i.e., $\partial u/\partial x + C = 0$ in $x = 0$ on one hand, and a constant flux of water J_0 in $x = 0$, i.e., $\partial C/\partial x = J_0/D$ in $x = 0$ and $C \rightarrow C_\infty$ for $x \rightarrow \infty$ on the other hand.

To solve the coupled set of Eqs. (1) and (2), we first consider the case when there is no water loss, $J_0 = 0$. The stress field then results solely from the crack opening and will correspond to $t = 0$. Using a Fourier decomposition on y , we find for the dimensionless stress $\Sigma_{xx} = \sigma_{xx}/\bar{E}C_\infty$:

$$\Sigma_{xx} = 1 - \frac{2}{\pi} \arctan\left(\frac{\sin\pi Y}{\sinh\pi X}\right), \quad (3)$$

where $X = x/e$ and $Y = y/e$. The variation of Σ_{xx} versus X for $Y = \frac{1}{2}$ corresponds to the curve $T = 0$ in Fig. 4. When $J_0 \neq 0$, Σ_{xx} involves three terms. The first is

related to the stress relaxation due to the presence of the crack, of the same form as [3], it increases with X . The second expresses the internal stress created by the water content variation when $u = 0$ everywhere, this term increases with time and decreases with X . The third is a correction of the second, taking into account that, after removing the crack, deformation occurs ($u \neq 0$) to counterbalance the nonuniformity of the internal stress. In practice, this last term is negligible and Σ_{xx} is given by

$$\Sigma_{xx} = \left[1 - \frac{2}{\pi} \left(1 + 2K\sqrt{\frac{T}{\pi}} \arctan\left(\frac{\sin\pi Y}{\sin\pi X}\right) \right) \right] + (2K\sqrt{T})i \operatorname{erfc}\left(\frac{X}{2\sqrt{T}}\right), \quad (4)$$

where T represents the dimensionless time $T = Dt/e^2$ and K the dimensionless flux of water content in $X = 0$, $K = J_0 e/DC_\infty$. First, we consider the case $K = 1$ (see Fig. 4). The variation of Σ_{xx} with X exhibits a maximum which increase with time. As a consequence, the next crack will preferentially form or grow near the first one. Furthermore, as shown by numerical calculations, the position of the maximum on X , Λ , is practically independent of T , leading to a well defined spacing between the cracks. When K is varied, the shape of $\Sigma_{xx}(X, T)$ changes. When K increases, as the flux of water increases (i.e., the absolute value of the slope in $X = 0$ of the second term of Σ_{xx}), the maximum is more pronounced and gets closer to $X = 0$. That results in a decrease of Λ . In contrast, when K decreases, the maximum flattens and Λ increases. Numerical calculations show, however, that the variation of Λ with K is very weak (see Fig. 5).

Let us now turn back to the experiments. The various runs were done under the same experimental conditions; K is simply proportional to e , so K varies over about a factor of 10. Consequently, $\Lambda = \lambda/e$ is expected to

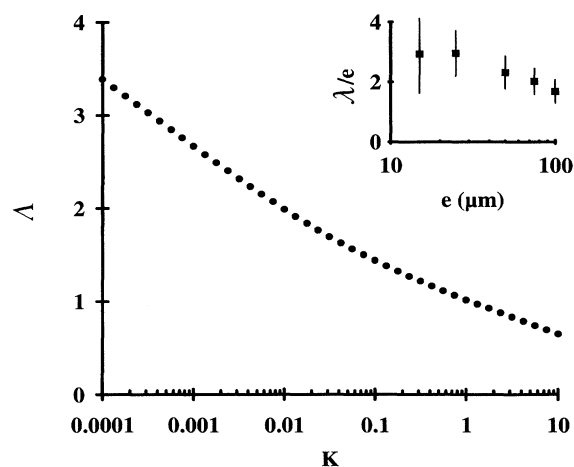


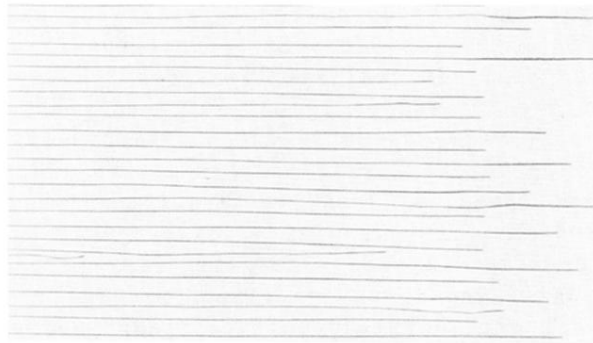
FIG. 5. Variation of the calculated dimensionless wavelength $\Lambda = \lambda/e$ as a function of $K = J_0 e/DC_\infty$. Inset: measured ratio λ/e as a function of e ; the bars are the errors in the measurements.

decrease slightly with e , good agreement is observed with the measured variation (see inset in Fig. 5). The direct comparison of the experimental data with the calculations requires knowledge of J_0 , D , and C_∞ . Their precise determination is tricky but rough estimates can be done. J_0 can be taken of the same order as the mean volume rate of water loss, from weighing measurements, we find $J_0 \cong 10^{-7} \text{ m s}^{-1}$. D is given by the product of the capillary characteristic velocity ($\cong \gamma/\eta$, where η is the water viscosity), and the hydraulic radius of the pore gel calculated from the expression of Kozeny-Carman [17], yielding $D \cong 3 \times 10^{-8} \text{ m}^2 \text{ s}^{-1}$. Finally, C_∞ can be estimated as a fraction of $\Delta\phi_w$: $C_\infty \cong 10^{-1}$. So we find, for $e = 100 \text{ }\mu\text{m}$, $K \cong 3 \times 10^{-3}$. For this value, our simplified model leads to $\Lambda \cong 2-3$ [15] which is consistent with the experimental values (see Fig. 5).

To conclude, we find that directional drying in a confined geometry leads to the formation of regular patterns of crack. We propose that the characteristic wavelength results from the competition between the stress relaxation due to crack opening and the stress increase due to water loss. Good agreement is found between the experimental values and estimates based on a simplified 2D scalar model. Further investigations on the dynamics will allow confirmation of our model and a gain in insight into the relation between this mechanical problem and other one-dimensional cellular systems.

We are grateful to M. Cloitre and I. Marsone for their help in the experiment and for valuable discussions.

- [1] *Statistical Models for the Fracture of Disordered Media*, edited by H.J. Hermann and S. Roux (North-Holland, Amsterdam, 1990).
- [2] *Disorder and Fracture*, edited by J.C. Charmet, S. Roux, and E. Guyon (Plenum Press, New York, 1990).
- [3] J.W. Hutchinson, *Adv. Appl. Mech.* **29**, 63 (1992).
- [4] P. Meakin, *Thin solid Films* **151**, 165 (1987).
- [5] S. Nemat-Nasser, L.M. Keer, and K.S. Parihar, *Int. J. Solids Structures* **14**, 409 (1978).
- [6] H.A. Bahr, H.J. Weiss, H.G. Maschke, and F. Meissner, *Theor. Appl. Fracture Mech.* **10**, 219 (1988).
- [7] J.S. Langer, *Phys. Rev. A* **46**, 3123 (1992).
- [8] A. Yuse and M. Sano, *Nature (London)* **362**, 329 (1993).
- [9] M. Marder, *Phys. Rev. E* **49**, R51 (1994).
- [10] Y. Hayakawa, *Phys. Rev. B* **49**, R1804 (1994).
- [11] J.M. Flesselles, A.J. Simon, and A.J. Libchaber, *Adv. Phys.* **40**, 1 (1991).
- [12] R.K. Iler, *The Chemistry of Silica* (John Wiley & Sons, New York, 1979).
- [13] C.J. Brinker and G.W. Scherer, *Sol-Gel Science* (Academic Press, New York, 1990), Chap. 8.
- [14] J. Zarzycki, *J. Non-Cryst. Solids* **100**, 359 (1988).
- [15] Under the assumptions used here, it is possible to develop a vectorial model. However, it does not change significantly the predicted values for the wavelength [L. Limat, unpublished].
- [16] A.V. Luikov, *Heat and Mass Transfer in Capillary-Porous Bodies* (Pergamon Press, London, 1966).
- [17] F.A.L. Dullien, *Porous Media: Fluid Transport and Pore Structure*, (Academic Press, San Diego, 1979).



(a)

→ crack growth direction



(b)

— 300 μm

FIG. 2. Top views of the crack pattern: (a) crack front invading the cell, (b) secondary branching, taken about 10 min later. The evaporation side is on the left. The cell thickness is $15 \mu\text{m}$.